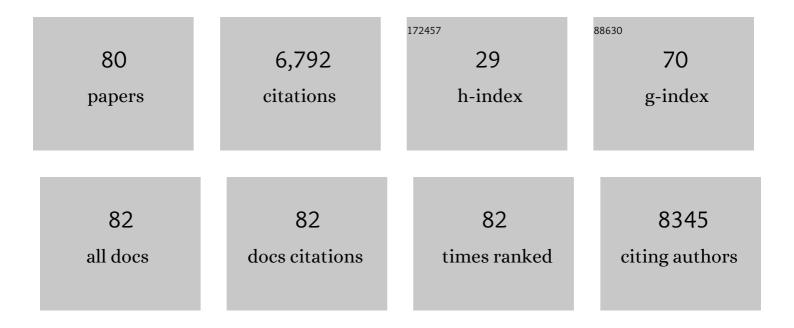
## Martin A Lodge

List of Publications by Year in descending order

Source: https://exaly.com/author-pdf/7623016/publications.pdf Version: 2024-02-01



#	Article	IF	CITATIONS
1	From RECIST to PERCIST: Evolving Considerations for PET Response Criteria in Solid Tumors. Journal of Nuclear Medicine, 2009, 50, 122S-150S.	5.0	3,047
2	Combretastatin A4 Phosphate Has Tumor Antivascular Activity in Rat and Man as Demonstrated by Dynamic Magnetic Resonance Imaging. Journal of Clinical Oncology, 2003, 21, 2831-2842.	1.6	328
3	Practical PERCIST: A Simplified Guide to PET Response Criteria in Solid Tumors 1.0. Radiology, 2016, 280, 576-584.	7.3	311
4	Biodistribution, Tumor Detection, and Radiation Dosimetry of <sup>18</sup> F-DCFBC, a Low-Molecular-Weight Inhibitor of Prostate-Specific Membrane Antigen, in Patients with Metastatic Prostate Cancer. Journal of Nuclear Medicine, 2012, 53, 1883-1891.	5.0	264
5	A PET study of 18 FDG uptake in soft tissue masses. European Journal of Nuclear Medicine and Molecular Imaging, 1999, 26, 22-30.	6.4	259
6	Noise Considerations for PET Quantification Using Maximum and Peak Standardized Uptake Value. Journal of Nuclear Medicine, 2012, 53, 1041-1047.	5.0	186
7	<sup>18</sup> F-DCFBC PET/CT for PSMA-Based Detection and Characterization of Primary Prostate Cancer. Journal of Nuclear Medicine, 2015, 56, 1003-1010.	5.0	180
8	Effects of 5,6-Dimethylxanthenone-4-Acetic Acid on Human Tumor Microcirculation Assessed by Dynamic Contrast-Enhanced Magnetic Resonance Imaging. Journal of Clinical Oncology, 2002, 20, 3826-3840.	1.6	150
9	Dynamic whole-body PET imaging: principles, potentials and applications. European Journal of Nuclear Medicine and Molecular Imaging, 2019, 46, 501-518.	6.4	145
10	Repeatability of SUV in Oncologic <sup>18</sup> F-FDG PET. Journal of Nuclear Medicine, 2017, 58, 523-532.	5.0	133
11	Human Biodistribution and Radiation Dosimetry of <sup>82</sup> Rb. Journal of Nuclear Medicine, 2010, 51, 1592-1599.	5.0	117
12	Feasibility of state of the art PET/CT systems performance harmonisation. European Journal of Nuclear Medicine and Molecular Imaging, 2018, 45, 1344-1361.	6.4	100
13	Dynamic imaging in patients with tuberculosis reveals heterogeneous drug exposures in pulmonary lesions. Nature Medicine, 2020, 26, 529-534.	30.7	87
14	<sup>124</sup> I PET-Based 3D-RD Dosimetry for a Pediatric Thyroid Cancer Patient: Real-Time Treatment Planning and Methodologic Comparison. Journal of Nuclear Medicine, 2009, 50, 1844-1847.	5.0	80
15	Radiation absorbed dose distribution in a patient treated with yttrium-90 microspheres for hepatocellular carcinoma. Medical Physics, 2004, 31, 2449-2453.	3.0	79
16	Combination of the histone deacetylase inhibitor vorinostat with bevacizumab in patients with clear-cell renal cell carcinoma: a multicentre, single-arm phase I/II clinical trial. British Journal of Cancer, 2017, 116, 874-883.	6.4	78
17	Noninvasive <sup>11</sup> C-rifampin positron emission tomography reveals drug biodistribution in tuberculous meningitis. Science Translational Medicine, 2018, 10, .	12.4	73
18	Radiation Dosimetry of <sup>82</sup> Rb in Humans Under Pharmacologic Stress. Journal of Nuclear Medicine, 2011, 52, 485-491.	5.0	68

MARTIN A LODGE

#	Article	IF	CITATIONS
19	Differences in Skeletal Kinetics Between Vertebral and Humeral Bone Measured by 18F-Fluoride Positron Emission Tomography in Postmenopausal Women. Journal of Bone and Mineral Research, 2010, 15, 763-769.	2.8	61
20	Physical aspects of yttrium-90 microsphere therapy for nonresectable hepatic tumors. Medical Physics, 2003, 30, 199-203.	3.0	59
21	The QIBA Profile for FDG PET/CT as an Imaging Biomarker Measuring Response to Cancer Therapy. Radiology, 2020, 294, 647-657.	7.3	49
22	Cardiac PET/CT Misregistration Causes Significant Changes in Estimated Myocardial Blood Flow. Journal of Nuclear Medicine, 2013, 54, 50-54.	5.0	43
23	Timed sequential therapy of the selective T-type calcium channel blocker mibefradil and temozolomide in patients with recurrent high-grade gliomas. Neuro-Oncology, 2017, 19, 845-852.	1.2	39
24	Potential novel application of dual time point SUV measurements as a predictor of survival in head and neck cancer. Nuclear Medicine Communications, 2005, 26, 861-867.	1.1	38
25	The effect of regadenoson on the integrity of the human blood–brain barrier, a pilot study. Journal of Neuro-Oncology, 2017, 132, 513-519.	2.9	38
26	Semiquantitative Parameters in PSMA-Targeted PET Imaging with <sup>18</sup> F-DCFPyL: Variability in Normal-Organ Uptake. Journal of Nuclear Medicine, 2017, 58, 942-946.	5.0	38
27	Reproducibility of Tumor Blood Flow Quantification with <sup>15</sup> O-Water PET. Journal of Nuclear Medicine, 2008, 49, 1620-1627.	5.0	35
28	Comparison of quantitative Yâ€90 SPECT and nonâ€timeâ€ofâ€flight PET imaging in postâ€therapy radioembolization of liver cancer. Medical Physics, 2016, 43, 5779-5790.	3.0	32
29	Optimization of Rb-82 PET acquisition and reconstruction protocols for myocardial perfusion defect detection. Physics in Medicine and Biology, 2009, 54, 3161-3171.	3.0	31
30	Comprehensive Radionuclide Esophagogastrointestinal Transit Study: Methodology, Reference Values, and Initial Clinical Experience. Journal of Nuclear Medicine, 2015, 56, 721-727.	5.0	31
31	Impact of <scp>PET</scp> / <scp>CT</scp> system, reconstruction protocol, data analysis method, and repositioning on <scp>PET</scp> / <scp>CT</scp> precision: An experimental evaluation using an oncology and brain phantom. Medical Physics, 2017, 44, 6413-6424.	3.0	30
32	Simultaneous measurement of noise and spatial resolution in PET phantom images. Physics in Medicine and Biology, 2010, 55, 1069-1081.	3.0	28
33	Dynamic Multi-Bed FDG PET imaging: Feasibility and optimization. , 2011, , .		28
34	Repeatability of <sup>18</sup> F-FLT PET in a Multicenter Study of Patients with High-Grade Glioma. Journal of Nuclear Medicine, 2017, 58, 393-398.	5.0	27
35	Semiquantitative Parameters in PSMA-Targeted PET Imaging with [18F]DCFPyL: Impact of Tumor Burden on Normal Organ Uptake. Molecular Imaging and Biology, 2020, 22, 190-197.	2.6	27
36	A Practical, Automated Quality Assurance Method for Measuring Spatial Resolution in PET. Journal of Nuclear Medicine, 2009, 50, 1307-1314.	5.0	26

MARTIN A LODGE

#	Article	IF	CITATIONS
37	Developments in nuclear cardiology: transition from single photon emission computed tomography to positron emission tomography-computed tomography. Journal of Invasive Cardiology, 2005, 17, 491-6.	0.4	26
38	Effect of Patient Arm Motion in Whole-Body PET/CT. Journal of Nuclear Medicine, 2011, 52, 1891-1897.	5.0	23
39	Liver Standardized Uptake Value Corrected for Lean Body Mass at FDG PET/CT. Clinical Nuclear Medicine, 2015, 40, e17-e22.	1.3	22
40	Biodistribution and Radiation Dosimetry of <sup>124</sup> I-DPA-713, a PET Radiotracer for Macrophage-Associated Inflammation. Journal of Nuclear Medicine, 2018, 59, 1751-1756.	5.0	22
41	Performance assessment of a NaI(Tl) gamma counter for PET applications with methods for improved quantitative accuracy and greater standardization. EJNMMI Physics, 2015, 2, .	2.7	18
42	Impact of acquisition time-window on clinical whole-body PET parametric imaging. , 2014, , .		16
43	A comparison of FLT to FDG PET/CT in the early assessment of chemotherapy response in stages IB–IIIA research, 2017, 7, 8.	2.5	16
44	Measuring PET Spatial Resolution Using a Cylinder Phantom Positioned at an Oblique Angle. Journal of Nuclear Medicine, 2018, 59, 1768-1775.	5.0	16
45	Dynamic PET-facilitated modeling and high-dose rifampin regimens for <i>Staphylococcus aureus</i> orthopedic implant–associated infections. Science Translational Medicine, 2021, 13, eabl6851.	12.4	16
46	Comparison of 2-dimensional and 3-dimensional acquisition for 18F-FDG PET oncology studies performed on an LSO-based scanner. Journal of Nuclear Medicine, 2006, 47, 23-31.	5.0	15
47	Simplifying volumesâ€ofâ€interest (VOIs) definition in quantitative SPECT: Beyond manual definition of 3D wholeâ€organ VOIs. Medical Physics, 2017, 44, 1707-1717.	3.0	14
48	Quantitative PET/CT in clinical practice. Nuclear Medicine Communications, 2018, 39, 154-160.	1.1	14
49	Semiquantitative Parameters in PSMA-Targeted PET Imaging with [18F]DCFPyL: Intrapatient and Interpatient Variability of Normal Organ Uptake. Molecular Imaging and Biology, 2020, 22, 181-189.	2.6	14
50	Imageâ€derived and arterial blood sampled input functions for quantitative PET imaging of the angiotensin II subtype 1 receptor in the kidney. Medical Physics, 2015, 42, 6736-6744.	3.0	13
51	Quantitative myocardial perfusion PET parametric imaging at the voxel-level. Physics in Medicine and Biology, 2015, 60, 6013-6037.	3.0	13
52	Impact of point spread function reconstruction on quantitative 18F-FDG-PET/CT imaging parameters and inter-reader reproducibility in solid tumors. Nuclear Medicine Communications, 2016, 37, 288-296.	1.1	12
53	Combined model-based and patient-specific dosimetry for 18F-DCFPyL, a PSMA-targeted PET agent. European Journal of Nuclear Medicine and Molecular Imaging, 2018, 45, 989-998.	6.4	12
54	Characterization of a Perirectal Artifact in <sup>18</sup> F-FDG PET/CT. Journal of Nuclear Medicine, 2010, 51, 1501-1506.	5.0	11

MARTIN A LODGE

#	Article	IF	CITATIONS
55	Introducing time-of-flight and resolution recovery image reconstruction to clinical whole-body PET parametric imaging. , 2014, , .		11
56	Human Radiation Dosimetry for Orally and Intravenously Administered <sup>18</sup> F-FDG. Journal of Nuclear Medicine, 2020, 61, 613-619.	5.0	11
57	18F-FDG PET of the hands with a dedicated high-resolution PEM system (arthro-PET): correlation with PET/CT, radiography and clinical parameters. European Journal of Nuclear Medicine and Molecular Imaging, 2014, 41, 2337-2345.	6.4	10
58	ACR–ASNR Practice Parameter for Brain PET/CT Imaging Dementia. Clinical Nuclear Medicine, 2016, 41, 118-125.	1.3	10
59	Impact of Tumor Burden on Quantitative [68Ga] DOTATOC Biodistribution. Molecular Imaging and Biology, 2019, 21, 790-798.	2.6	10
60	Methodology for quantifying absolute myocardial perfusion with PET and SPECT. Current Cardiology Reports, 2007, 9, 121-128.	2.9	9
61	Resolution modeled PET image reconstruction incorporating space-variance of positron range: Rubidium-82 cardiac PET imaging. , 2008, , .		9
62	Comparison of two software systems for quantification of myocardial blood flow in patients with hypertrophic cardiomyopathy. Journal of Nuclear Cardiology, 2019, 26, 1243-1253.	2.1	8
63	Repeatability of Radiotracer Uptake in Normal Abdominal Organs with <sup>111</sup> In-Pentetreotide Quantitative SPECT/CT. Journal of Nuclear Medicine, 2015, 56, 985-988.	5.0	7
64	Measuring temporal stability of positron emission tomography standardized uptake value bias using long-lived sources in a multicenter network. Journal of Medical Imaging, 2018, 5, 1.	1.5	7
65	An Exocrine Pancreatic Stress Test with <sup>11</sup> C-Acetate PET and Secretin Stimulation. Journal of Nuclear Medicine, 2014, 55, 1128-1131.	5.0	6
66	ACR–SPR–STR Practice Parameter for the Performance of Cardiac Positron Emission Tomography - Computed Tomography (PET/CT) Imaging. Clinical Nuclear Medicine, 2017, 42, 918-927.	1.3	6
67	Prospective Within-Patient Assessment of the Impact of an Unlabeled Octreotide Pre-dose on the Biodistribution and Tumor Uptake of 68Ga DOTATOC as Assessed by Dynamic Whole-body PET in Patients with Neuroendocrine Tumors: Implications for Diagnosis and Therapy. Molecular Imaging and Biology, 2021, 23, 766-774.	2.6	6
68	Effect of Point-Spread Function Reconstruction for Indeterminate PSMA-RADS-3A Lesions on PSMA-Targeted PET Imaging of Men with Prostate Cancer. Diagnostics, 2021, 11, 665.	2.6	6
69	High SUVs Have More Robust Repeatability in Patients with Metastatic Prostate Cancer: Results from a Prospective Test-Retest Cohort Imaged with <sup>18</sup> F-DCFPyL. Molecular Imaging, 2022, 2022, 7056983.	1.4	6
70	Generation and evaluation of a simultaneous cardiac and respiratory gated Rb-82 PET simulation. , 2011, 2011, 3327-3330.		5
71	Quantitative whole-body parametric PET imaging incorporating a generalized Patlak model. , 2013, , .		5
72	Imager-4D: New Software for Viewing Dynamic PET Scans and Extracting Radiomic Parameters from PET Data. Journal of Digital Imaging, 2019, 32, 1071-1080.	2.9	5

#	Article	IF	CITATIONS
73	Enhanced whole-body PET parametric imaging using hybrid regression and thresholding driven by kinetic correlations. , 2012, , .		4
74	Clinical evaluation of direct 4D whole-body PET parametric imaging with time-of-flight and resolution modeling capabilities. , 2015, , .		3
75	The Unique Role of Fluorodeoxyglucose-PET in Radioembolization. PET Clinics, 2019, 14, 447-457.	3.0	3
76	Measurement of PET Quantitative Bias In Vivo. Journal of Nuclear Medicine, 2021, 62, 732-737.	5.0	3
77	Parametric myocardial perfusion PET imaging using physiological clustering. Proceedings of SPIE, 2014, , .	0.8	2
78	Phantom Preparation Using a Dilution Technique. Journal of Nuclear Medicine, 2021, 62, 303-303.	5.0	1
79	Letter to the Editor re: "Semiquantitative Parameters in PSMA-Targeted PET Imaging with [18F]DCFPyL: Impact of Tumor Burden on Normal Organ Uptake― Molecular Imaging and Biology, 2020, 22, 19-21.	2.6	0
80	Quantitative Imaging in Oncologic PET. , 2021, , 1-100.		0